Journal of
Mechanics of
Materials and Structures

WAVE SCATTERING FROM A RECTANGULAR CRACK IN AN ANISOTROPIC CLADDING

Per-Åke Jansson

Volume 6, No. 9-10 November–December 2011

mathematical sciences publishers

JOURNAL OF MECHANICS OF MATERIALS AND STRUCTURES
Vol. 6, No. 9-10, 2011

WAVE SCATTERING FROM A RECTANGULAR CRACK IN AN ANISOTROPIC CLADDING

PER-ÅKE JANSSON

Ultrasonic testing of a thick elastic plate with a crack in an anisotropic cladding is modeled analytically for a fully three-dimensional case. The model includes an ultrasonic transmitter and a receiver as well as wave scattering from a rectangular crack. The effect of a corrugated interface between the base component and the cladding is also taken into account. To solve the scattering problem the null field approach is employed to determine a Green's tensor for the same structure without a crack and the source point located in the cladding. Utilizing the Green's tensor an integral representation for the displacement field in the same structure with a crack and an incident field generated by an ultrasonic transducer may be derived. It is then straightforward to derive a hypersingular integral equation for the crack opening displacement, which can be used to determine the change in signal response due to the crack by Auld's reciprocity argument. Numerical results are given for a variety of cases illustrating the effects of size, position, and orientation of the crack and the properties of the corrugated interface.

Introduction

Ultrasonic nondestructive testing is frequently used to detect defects, e.g., in nuclear power plants. Even though the method has been in use for a considerable time and may be regarded as well-established, there is a need for modeling of the testing procedure. Such a model may be useful for planning of testing, for qualification of testing procedures, for interpretation of results, and for education purposes. Using a good mathematical model also has the benefit of being much cheaper than experimental methods, in particular when parameter studies are performed.

In the nuclear power industry it is common to use claddings, i.e., layers of austenitic steel, to prevent or reduce corrosion. A cladding may be applied to a thick plate or a thick-walled pipe by a manual or automated welding process. As a result of the fabrication process the interface between the base material and the cladding usually becomes corrugated, which is likely to affect the propagation of ultrasonic waves. Furthermore, the cladding material is normally anisotropic, which will also complicate the interpretation of test results. Thus, a numerical model for the testing procedure may be useful for understanding of the influence of the cladding on the signal response. An overview of ultrasonic testing of clad components is given in [Hudgell 1994].

Various wave propagation problems for a thick plate with a cladding with or without a crack have been studied previously. The 2D and 3D wave propagation problems for a structure without a crack have been investigated in [Krasnova et al. 2005; Krasnova 2005] using the null field approach, and in [Krasnova and Jansson 2006] using approximate boundary conditions at the interface. The 2D scalar scattering problem with a strip-like crack was solved in [Zagbai and Boström 2006], and the 2D P-SV

Keywords: ultrasound, crack, anisotropy, cladding.

problem in [Jansson and Zagbai 2007]. In the present paper the analysis is generalized to the 3D case. A rudimentary version has previously been presented at a conference [Jansson 2010].

The aim of this paper is to develop a fully three-dimensional analytical model for a thick plate with a rectangular crack of arbitrary orientation in a cladding. Both materials are allowed to be anisotropic without any restrictions on symmetry or orientation of the crystal axes. In the numerical examples, however, only the case of an isotropic base material and a transversely isotropic cladding is studied. The effect of a one-dimensionally periodic interface between the base component and the cladding is also taken into account. Actually, real interfaces for welded claddings are more or less periodic. Besides, the analysis will be considerably simplified, since the periodicity can be utilized to discretize the problem. To solve the scattering problem a hypersingular integral equation technique is employed. The solution is exact in the sense that no restrictions are imposed on the frequency of the ultrasonic transmitter or the shape of the periodic interface, although numerical results are only given for a sinusoidal surface. In practice, however, the convergence will be poor for high frequencies and very rough interfaces. The results are believed to be valid, at least qualitatively, not only for a plate but also for components with curved surfaces, like pressure vessels and pipes, as long as the curvature is sufficiently small.

The integral equation method used in this paper is computationally efficient, but has the drawback that only defects of simple shapes can be handled. For more complex geometries it is necessary to rely on other methods, such as the finite element method. However, for 3D geometries and high frequencies a very large number of elements is needed, which may be a limitation. Other numerical methods include the strip element method of [Liu and Achenbach 1995], the elastodynamic finite integration technique, or EFIT [Langenberg et al. 2000], and the boundary element method (see [Wang et al. 1996], for example). Elastic wave scattering from periodic surfaces have previously been studied extensively for the case of isotropic media; see, e.g., [Fokkema and van den Berg 1977; Fokkema 1980; Lakhtakia et al. 1984].

1. Problem formulation

The geometry of the wave propagation problem is depicted in Figure 1. A thick plate is composed of two layers of different generally anisotropic materials in welded contact. The crystal axes may be arbitrarily

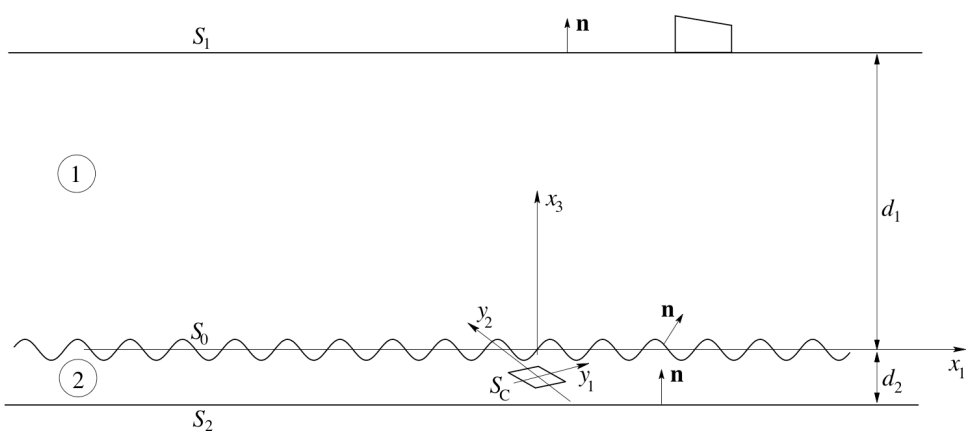

Figure 1. The geometry of a plate with a crack inside a cladding.

oriented. The interface S_0 is assumed to be periodic with a period a. This is believed to be a reasonable approximation, since real interfaces are more or less periodic. The layer of thickness d_1 is the base material. The cladding of thickness d_2 contains a rectangular crack

$$S_C \quad (|y_1| < c, |y_2| < d),$$

which may be tilted arbitrarily with respect to the back wall S_2. An ultrasonic transmitter is placed on the free surface S_1 of the base material. All numerical examples given here are for a transducer working in pulse-echo mode, even though the analysis is valid for the case of tandem inspection as well. Only the case of a transducer working at a fixed angular frequency ω will be considered, although it is straightforward, but somewhat time-consuming, to obtain results in the time domain.

For time-harmonic conditions the displacement fields u^i_j in the two materials $i = 1, 2$ satisfy

$$\frac{\partial}{\partial x_k}\sigma^i_{kj} + \rho^i \omega^2 u^i_j = 0, \tag{1}$$

where ρ^i is the corresponding density, and σ^i_{kj} is the stress tensor, which is related to the displacement by the constitutive relation

$$\sigma^i_{kj} = c^i_{kjk'j'} \frac{\partial}{\partial x_{j'}} u^i_{k'}, \tag{2}$$

where $c^i_{kjk'j'}$ are the stiffnesses of material i. Unless otherwise stated the summation convention is used throughout in the following.

The boundary conditions to be satisfied are

$$t_j = \sigma_{kj} n_k = 0$$

on S_1 (except directly below the transducer), S_2, and S_C. Furthermore, u_j and t_j are continuous on the interface S_0, where $x_3 = s(x_1)$. Here $s(x_1)$ is assumed to be a periodic function; in fact, it is taken as sinusoidal in the numerical examples:

$$s(x_1) = b \sin \frac{2\pi x_1}{a}. \tag{3}$$

There are two main reasons for this. Firstly, real interfaces are more or less sinusoidal. Secondly, certain integrals that will appear during the analysis can be evaluated analytically, which will speed up the computations considerably. It should be pointed out, however, that there is no fundamental difficulty in choosing some other periodic function, as long as it is differentiable. Finally, it is assumed that the radiation conditions are fulfilled, so that all waves are outgoing at infinity.

The first step in the solution is to determine a Green's tensor for the same structure without a crack. The source point is located in the cladding. This tensor is then used to derive an integral representation for the displacement field in the same structure with a crack and an incident field generated by an ultrasonic transducer. From the integral representation it is then possible to derive a hypersingular integral equation for the crack opening displacement. Once the crack opening displacement is known the change in signal response due to the crack can be determined using Auld's reciprocity argument [1979].

2. The Green's tensor for the structure without a crack

To determine the Green's tensor for the layered plate without a crack with a source in the cladding, i.e., the displacement field in both materials caused by a point force in material 2, the following integral representations are used:

$$\int_{S_1-S_0} \left[\Sigma_{kjj'}(\boldsymbol{x};\boldsymbol{x}')G^1_{jj''}(\boldsymbol{x};\boldsymbol{x}'') - G_{jj'}(\boldsymbol{x};\boldsymbol{x}')\Sigma^1_{kjj''}(\boldsymbol{x};\boldsymbol{x}'')\right]n_k \,\mathrm{d}S = \begin{cases} G_{j''j'}(\boldsymbol{x}'';\boldsymbol{x}') & (\boldsymbol{x}'' \text{ in material 1}), \\ 0 & (\boldsymbol{x}'' \text{ in material 2}); \end{cases} \tag{4}$$

$$\int_{S_0-S_2} \left[\Sigma_{kjj'}(\boldsymbol{x};\boldsymbol{x}')G^2_{jj''}(\boldsymbol{x};\boldsymbol{x}'') - G_{jj'}(\boldsymbol{x};\boldsymbol{x}')\Sigma^2_{kjj''}(\boldsymbol{x};\boldsymbol{x}'')\right]n_k \,\mathrm{d}S = \begin{cases} -G^2_{j''j'}(\boldsymbol{x}'';\boldsymbol{x}') & (\boldsymbol{x}'' \text{ in material 1}), \\ -G^2_{j''j'}(\boldsymbol{x}'';\boldsymbol{x}') + G_{j''j'}(\boldsymbol{x}'';\boldsymbol{x}'). & (\boldsymbol{x}'' \text{ in material 2}). \end{cases} \tag{5}$$

Here $G_{jj'}(\boldsymbol{x};\boldsymbol{x}')$ is the Green's tensor to be determined, and $G^i_{jj'}(\boldsymbol{x};\boldsymbol{x}')$ are half-space Green's tensors for material $i = 1, 2$. If the scattering properties of the interface are considered, $G^2_{j''j'}$ may be regarded as an incident field, $G_{j''j'}$ as the scattered field in material 1, and $G_{j''j'} - G^2_{j''j'}$ as the scattered field in material 2. The corresponding stress tensors $\Sigma^i_{kjj'}$ are related to the Green's tensors by

$$\Sigma^i_{kjj'}(\boldsymbol{x};\boldsymbol{x}') = c^i_{kjk'j''}\frac{\partial}{\partial x_{j''}}G^i_{k'j'}(\boldsymbol{x};\boldsymbol{x}'). \tag{6}$$

The half-space Green's tensors can be expressed as double Fourier transforms in x_1 and x_2:

$$G^2_{jj'}(\boldsymbol{x};\boldsymbol{x}') = \int_{-\infty}^{\infty}\int_{-\infty}^{\infty}\sum_{n=1}^{3} D^{2\pm}_n U^{2\pm}_{nj'}U^{2\pm}_{nj}\,\mathrm{e}^{\mathrm{i}(q(x_1-x_1')+p(x_2-x_2')+h^{2\pm}_n(x_3-x_3'))}\,\mathrm{d}q\,\mathrm{d}p + \int_{-\infty}^{\infty}\int_{-\infty}^{\infty}\sum_{n,n'=1}^{3} D^{2-}_n U^{2-}_{nj'}B^2_{nn'}U^{2+}_{n'j}\,\mathrm{e}^{\mathrm{i}(q(x_1-x_1')+p(x_2-x_2')+h^{2+}_{n'}(x_3+d_2)-h^{2-}_n(x_3'+d_2))}\,\mathrm{d}q\,\mathrm{d}p, \tag{7}$$

for $x_3 \gtrless x_3'$, and similarly for $G^1_{jj'}$; see Appendix A. Here $U^{2\pm}_{nj}$ are polarization vectors and $h^{2\pm}_n$ are the corresponding wavenumbers in the x_3-direction for plane wave solutions. These can be determined from a generalized eigenvalue problem derived from (1) and (2). The + and − signs refer to up- and downgoing waves, respectively. The coefficients $D^{2\pm}_n$ are determined from the jump condition at $x_3 = x_3'$, and $B^2_{nn'}$ is a reflection matrix determined from the condition of vanishing traction at the free surface S_2. The details are given in Appendix A.

The scattered field in material 2 may be expanded as

$$G_{jj'}(\boldsymbol{x};\boldsymbol{x}') - G^2_{jj'}(\boldsymbol{x};\boldsymbol{x}') = \int_{-\infty}^{\infty}\int_{-\infty}^{\infty}\sum_{n=1}^{3} f_{nj'}(q,\,p;\,x_1',\,x_2',\,x_3')[U^{2-}_{nj}\,\mathrm{e}^{\mathrm{i}(qx_1+px_2+h^{2-}_n x_3)} + \sum_{n,n'=1}^{3} B^2_{nn'}U^{2+}_{n'j}\,\mathrm{e}^{\mathrm{i}(qx_1+px_2+h^{3+}_{n'}(x_3+d_2)-h^{2-}_n d_2)}]\,\mathrm{d}q\,\mathrm{d}p. \tag{8}$$

The surface fields $G_{jj'}$ and $\Sigma_{kjj'n_k}$ at the interface can also be expanded as Fourier transforms:

$$\begin{aligned} G_{jj'}(x_1, x_2, s(x_1); \boldsymbol{x}') &= \int_{-\infty}^{\infty}\int_{-\infty}^{\infty} \alpha_{jj'}(q', p'; \boldsymbol{x}')\mathrm{e}^{\mathrm{i}(q'x_1+p'x_2)}\,\mathrm{d}q'\,\mathrm{d}p', \\ \Sigma_{kjj'}(x_1, x_2, s(x_1); \boldsymbol{x}')(1+s'(x_1)^2)^{1/2}n_k &= \int_{-\infty}^{\infty}\int_{-\infty}^{\infty} \beta_{jj'}(q', p'; \boldsymbol{x}')\mathrm{e}^{\mathrm{i}(q'x_1+p'x_2)}\,\mathrm{d}q'\,\mathrm{d}p'. \end{aligned} \tag{9}$$

The factor $(1+s'^2)^{1/2}$ that appears in the integration measure is incorporated into the surface field for later convenience. To proceed the Fourier expansions for the Green's tensors and the surface fields are inserted into the integral representations (4)–(5), noting that $G_{jj'}(\boldsymbol{x}; \boldsymbol{x}') = G_{j'j}(\boldsymbol{x}'; \boldsymbol{x})$. Since the interface is periodic, the infinite integrals over the interface S_0 in (4) and (5) can be reduced to integrals over one period by using the identity

$$\int_{-\infty}^{\infty} g(x)\mathrm{e}^{\mathrm{i}qx}\,\mathrm{d}x = \sum_{l=-\infty}^{\infty} \delta\Big(\frac{qa}{2\pi}+l\Big)\int_0^a g(x)\mathrm{e}^{\mathrm{i}qx}\,\mathrm{d}x, \tag{10}$$

where $g(x)$ is periodic with period a; see [Richtmyer 1981], for instance.

After some tedious algebra a set of simultaneous equations for the Fourier coefficients is obtained:

$$\begin{aligned} 0 &= \sum_{l'=-\infty}^{\infty} \big(Q^1_{nlj'l'}\alpha_{j'jl'} + Q^2_{nlj'l'}\beta_{j'jl'}\big), \\ -\eta_{njl} &= \sum_{l'=-\infty}^{\infty} \big(Q^3_{nlj'l'}\alpha_{j'jl'} + Q^4_{nlj'l'}\beta_{j'jl'}\big), \\ f_{njl} &= \sum_{l'=-\infty}^{\infty} \big(P^3_{nlj'l'}\alpha_{j'jl'} + P^4_{nlj'l'}\beta_{j'jl'}\big), \end{aligned} \tag{11}$$

together with an equation for the Fourier coefficients of the scattered field in material 1, that will not be needed in the following. Here

$$f_{njl}(q_0, p) = f_{nj}(q_0 + 2l\pi/a, p) = f_{nj}(q, p)$$

with $|q_0| < \pi/a$, etc. The coefficients η_{nj} are expansion coefficients for the incident field, i.e., for the half-space Green's tensor in material 2:

$$\eta_{nj}(q, p; \boldsymbol{x}') = D^{2+}_n U^{2+}_{nj}\mathrm{e}^{-\mathrm{i}(qx'_1+px'_2+h^{2+}_n x'_3)} + \sum_{n'=1}^{3} D^{2-}_{n'} U^{2-}_{n'j} B^2_{n'n}\mathrm{e}^{-\mathrm{i}(qx'_1+px'_2h^{2+}_n d_2+h^{2-}_{n'}(x'_3+d_2))}. \tag{12}$$

Explicit expressions for the matrices P^i and Q^i are given in Appendix B for the case of a sinusoidal interface. From (11) it is now possible to solve for the coefficients f_{njl}, which means that the Green's tensor $G_{jj'}$ is determined in material 2. Introducing a matrix A such that

$$f_{njl} = \sum_{n'=1}^{3}\sum_{l'=-\infty}^{\infty} A_{nln'l'}\eta_{n'jl'}, \tag{13}$$

the explicit expression for the Green's tensor is

$$G_{jj'}(\boldsymbol{x};\boldsymbol{x}') = G^2_{jj'}(\boldsymbol{x};\boldsymbol{x}')$$
$$+ \sum_{l,l'=-\infty}^{\infty} \int_{-\pi/a}^{\pi/a} \int_{-\infty}^{\infty} \sum_{n=1}^{3} \left[U^{2-}_{njl} \mathrm{e}^{\mathrm{i}h^{2-}_{nl}x_3} + \sum_{n'=1}^{3} B^2_{nn'l} U^{2+}_{n'jl} \mathrm{e}^{\mathrm{i}[h^{2+}_{n'l}(x_3+d_2)-h^{2-}_{nl}d_2]} \right] \mathrm{e}^{\mathrm{i}(q_l x_1 + p x_2)} \sum_{n''=1}^{3} A_{nln''l'}$$
$$\times \left[D^{2+}_{n''l'} U^{2+}_{n''j'l'} \mathrm{e}^{-\mathrm{i}h^{2+}_{n''l'}x'_3} + \sum_{n'''=1}^{3} D^{2-}_{n'''l'} U^{2-}_{n'''j'l'} B^2_{n'''n''l'} \mathrm{e}^{\mathrm{i}(h^{2+}_{n''l'}d_2 - h^{2-}_{n'''l'}(x'_3+d_2))} \right] \times \mathrm{e}^{-\mathrm{i}(q_{l'}x'_1 + p x'_2)} \,\mathrm{d}q_0 \,\mathrm{d}p, \quad (14)$$

where $q_l = q_0 + 2l\pi/a$.

3. The integral equation for the crack opening displacement

In order to derive an integral equation for the crack opening displacement it is convenient to first transform the Green's stress tensor derived in the previous section to the crack coordinate system $y_1y_2y_3$; see Figure 1. Denoting the coordinates of the center of the crack by $(a_c,\ 0,\ -d_c)$ and introducing a rotation matrix R, the coordinate transformation is

$$x_1 = R_{1j}y_j + a_c, \quad x_2 = R_{2j}y_j, \quad x_3 = R_{3j}y_j - d_c. \quad (15)$$

The transformed Green's tensor is

$$G^{\mathrm{c}}_{jj'}(y_1, y_2, y_3; y'_1, y'_2, y'_3)$$
$$= \int_{-\infty}^{\infty}\int_{-\infty}^{\infty} \sum_{n=1}^{3} D^{\mathrm{c}\pm}_n U^{\mathrm{c}\pm}_{nj} U^{\mathrm{c}\pm}_{nj'} \mathrm{e}^{\mathrm{i}[q(y_1-y'_1)+p(y_2-y'_2)+h^{2+}_n(y_3-y'_3)]} \,\mathrm{d}q \,\mathrm{d}p$$
$$+ \int_{-\infty}^{\infty}\int_{-\infty}^{\infty} \sum_{n=1}^{3}\sum_{n'=1}^{3} D^{2-}_n U^{2\mathrm{c}-}_{nj'} B^2_{nn'} U^{2\mathrm{c}+}_{n'j} \mathrm{e}^{\mathrm{i}[\lambda^+_{kn'}y_k - \lambda^-_{kn'}y'_k + (h^{2+}_{n'} - h^{2-}_n)(d_2-d_{\mathrm{c}})]} \,\mathrm{d}q \,\mathrm{d}p$$
$$+ \sum_{l,l'=-\infty}^{\infty} \int_{-\pi/a}^{\pi/a} \int_{-\infty}^{\infty} \sum_{n=1}^{3} \left(U^{2\mathrm{c}-}_{njl} \mathrm{e}^{\mathrm{i}(\lambda^-_{knl}y_k - h^{2-}_{nl}d_{\mathrm{c}})} + \sum_{n'=1}^{3} B^{2\mathrm{c}+}_{nn'l} \mathrm{e}^{\mathrm{i}[\lambda^+_{kn'l}y_k + h^{2+}_{n'l}(d_2-d_{\mathrm{c}}) - h^{2-}_{nl}d_2]} \right)$$
$$\times \mathrm{e}^{\mathrm{i}q_l a_{\mathrm{c}}} \sum_{n''=1}^{3} A_{nln''l'} \left(\sum_{n'''=1}^{3} D^{2-}_{n'''l'} U^{2\mathrm{c}-}_{n'''j'l'} B^2_{n''n'''l'} \mathrm{e}^{-\mathrm{i}[\lambda^-_{k'n'''l'}y'_{k'} - h^{2-}_{n'''l'}d_2 + h^{2-}_{n'''l'}(d_2-d_{\mathrm{c}})]} \right.$$
$$\left. + D^{2+}_{n''l'} U^{2\mathrm{c}+}_{n''j'l'} \mathrm{e}^{-\mathrm{i}(\lambda^+_{k'n''l'}y'_{k'} - h^{2+}_{n''l'}d_{\mathrm{c}})} \right) \mathrm{e}^{-\mathrm{i}q_{l'}a_{\mathrm{c}}} \,\mathrm{d}q_0 \,\mathrm{d}p, \quad (16)$$

for $y_3 \gtrless y'_3$. Here

$$\lambda^{\pm}_{kn} = R_{1k}q + R_{2k}p + R_{3k}h^{\pm}_n, \quad (17)$$
$$U^{2\mathrm{c}\pm}_{nj} = R_{jj'}U^{\pm}_{nj}. \quad (18)$$

Since the free space part of the Green's function has the same expression in both systems, $D^{\mathrm{c}\pm}_n$ and $U^{\mathrm{c}\pm}_{nj}$ are determined in the same way as the corresponding quantities in the $x_1x_2x_3$-system using the appropriate stiffnesses, see Appendix A.

The corresponding stress tensor $\Sigma^{\mathrm{c}}_{kjj'}(\boldsymbol{x};\boldsymbol{x}')$ is given by

$$\Sigma^{\mathrm{c}}_{kjj'}(\boldsymbol{x};\boldsymbol{x}') = c^{2\mathrm{c}}_{kjk'j''}\frac{\partial}{\partial x_{j''}}G^{\mathrm{c}}_{k'j'}(\boldsymbol{x};\boldsymbol{x}'), \tag{19}$$

where $c^{2\mathrm{c}}_{kjk'j''}$ are the stiffnesses of material 2 in the crack coordinate system.

Starting from the Green's tensor an integral representation for the crack opening displacement $\Delta u_j(\mathbf{x})$ can be derived:

$$\int_{S_{\mathrm{c}}} \Delta u^{\mathrm{c}}_j(\boldsymbol{x})\Sigma^{\mathrm{c}}_{kjj'}(\boldsymbol{x};\boldsymbol{x}')n^{\mathrm{c}}_k \mathrm{d}S_{\mathrm{c}} = -u^{\mathrm{inc},2\mathrm{c}}_{j'}(\boldsymbol{x}') + u^{2\mathrm{c}}_{j'}(\boldsymbol{x}'). \tag{20}$$

Here superscript c denotes components in the crack system, and $u^{\mathrm{inc},2\mathrm{c}}_{j'}(\boldsymbol{x}')$ is the displacement field that would have existed in material 2 if the crack had not been there. This field was determined in [Krasnova et al. 2005; Krasnova 2005] using a model for the ultrasonic transducer, where the stress below the transducer is prescribed; see next section.

Operating once more with the traction operator, this time with respect to the field point $\boldsymbol{x}'$ and taking the limit as y'_3 approaches zero yield an integral equation for the crack opening displacement:

$$\lim_{y'_3\to 0^+}\int_{S_{\mathrm{c}}} \Delta u_j(y_1, y_2)\tau_{jj'}(y_1, y_2, 0; y'_1, y'_2, y'_3)\,\mathrm{d}S_{\mathrm{c}} = -\sigma^{\mathrm{inc},2\mathrm{c}}_{3j'}(y'_1, y'_2, 0) \tag{21}$$

Here $\tau_{jj'}$ is the double Green's stress tensor, and $\sigma^{\mathrm{inc},2\mathrm{c}}_{3j'}$ are stress components in the crack system due to the incident field. The explicit expression for $\tau_{jj'}$ is obtained by replacing $U^{\mathrm{c}\pm}_{nj}$, $U^{2\mathrm{c}\pm}_{nj}$, and $U^{2\mathrm{c}\pm}_{njl}$ in (16) by $S^{\pm}_{nj}$, $S^{2\mathrm{c}\pm}_{nj}$, and $S^{2\mathrm{c}\pm}_{njl}$, respectively, where

$$S^{\mathrm{c}\pm}_{nj} = \mathrm{i}(c^{2\mathrm{c}}_{3j1j'}q + c^{2\mathrm{c}}_{3j2j'}p + c^{2\mathrm{c}}_{3j3j'}h^{2\pm}_n)U^{\mathrm{c}\pm}_{nj'}, \tag{22}$$

$$S^{2\mathrm{c}\pm}_{nj} = \mathrm{i}c^{2\mathrm{c}}_{3jlj'}\lambda^{\pm}_{ln}U^{2\mathrm{c}\pm}_{nj'}, \tag{23}$$

$$S^{2\mathrm{c}\pm}_{njl} = \mathrm{i}c^{2\mathrm{c}}_{3jkj'}\lambda^{\pm}_{knl}U^{2\mathrm{c}\pm}_{nj'l}. \tag{24}$$

Equation (21) is hypersingular as a consequence of the twice differentiated Green's tensor. The limit in front cannot therefore be moved inside the integrand.

4. The incoming field

In the numerical examples only the case of an isotropic base material is studied. For this reason a transducer model developed in [Boström and Wirdelius 1995] is employed. In this model the stress at the interface between the transducer and the component is prescribed. It should be mentioned that there is no fundamental difficulty in treating an anisotropic base material, for instance by using the transducer model of [Niklasson 1998]. The explicit expression for the displacement field generated in an isotropic half-space is

$$u^{\mathrm{t}}_j = \int_{-\infty}^{\infty}\int_{-\infty}^{\infty}\sum_{n=1}^{3}\xi_n(q,p)U^{1-}_{nj}\mathrm{e}^{\mathrm{i}[q(x_1-x_{\mathrm{t}})+p(x_2-y_{\mathrm{t}})+h^{1-}_n(x_3-d_1)]}\,\mathrm{d}q\,\mathrm{d}p. \tag{25}$$

Here (x_t, y_t, d_1) are the coordinates of the transmitter, and the coefficients ξ_n are given in [Boström and Wirdelius 1995] for various types of transmitters. The displacement field in a cladding without a crack is

$$u_j^{\text{inc}} = \sum_{l=-\infty}^{\infty} \sum_{n=1}^{3} \int_{-\pi/a}^{\pi/a} \int_{-\infty}^{\infty} g_{nl} \left(U_{njl}^{2-} e^{ih_{nl}^{2-} x_3} + \sum_{n'=1}^{3} B_{nn'l}^{2} U_{n'jl}^{2+} e^{i[h_{n'l}^{2+}(x_3+d_3) - h_{nl}^{2-} d_2]} \right) e^{i(q_l x_1 + p x_2)} \, dq_0 \, dp, \quad (26)$$

according to [Krasnova et al. 2005; Krasnova 2005]. Here the coefficients g_{nl} are solutions to

$$\begin{cases} \sum_{l'=-\infty}^{\infty} \left(Q_{nljl'}^{1} \alpha_{jl'} + Q_{nljl'}^{2} \beta_{jl'} \right) = \xi_{nl} e^{-i(q_l x_t + p y_t + h_{nl}^{1-} d_1)}, \\ \sum_{l'=-\infty}^{\infty} \left(Q_{nljl'}^{3} \alpha_{jl'} + Q_{nljl'}^{4} \beta_{jl'} \right) = 0, \\ \sum_{l'=-\infty}^{\infty} \left(P_{nljl'}^{3} \alpha_{jl'} + P_{nljl'}^{4} \beta_{jl'} \right) = g_{nl}. \end{cases} \quad (27)$$

Transforming to the crack coordinate system, and operating with the traction operator, the right hand side of (21) is obtained.

5. Solution to the integral equation

To discretize the integral equation, the crack opening displacement is expanded in Chebyshev functions ϕ_m according to

$$\Delta u_j(y_1, y_2) = \sum_{m,m'=1}^{\infty} \gamma_{jmm'} \phi_m(y_1/c) \phi_{m'}(y_2/d), \quad (28)$$

where c, d are half the sides of the crack, and the expansion functions are defined as

$$\phi_m(s) = \begin{cases} \dfrac{1}{\pi} \cos(m \arcsin s) & \text{for } m = 1, 3, \ldots, \\ \dfrac{i}{\pi} \sin(m \arcsin s) & \text{for } m = 2, 4, \ldots. \end{cases} \quad (29)$$

It is convenient to choose the Chebyshev functions, since they form a complete set that exhibits, like the displacement field, a square root behavior at the crack tips. Furthermore, the functions have the pleasant property that

$$\int_{-c}^{c} \phi_m(y_1/c) e^{iq y_1} \, dy_1 = (-1)^{m+1} m \frac{J_m(qc)}{q}. \quad (30)$$

Inserting the expression for Δu_j into (21) and projecting the result onto the Chebyshev functions yield a linear system of equations for the unknowns $\gamma_{jmm'}$:

$$\sum_{j'=1}^{3} \sum_{m''=1}^{\infty} \sum_{m'''=1}^{\infty} Z_{jmm'j'm''m'''} \gamma_{j'm''m'''} = M_{jmm'} \quad (31)$$

The explicit expressions for the matrices Z and M are given in Appendix C. It is now straightforward to solve for the coefficients $\gamma_{jmm'}$. Hence, the crack opening displacement is determined.

6. The signal response

Next, the reciprocity result of [Auld 1979] is used to relate the crack opening displacement (COD) to the output voltage from the receiving probe:

$$\delta\Gamma_1 = -\frac{\mathrm{i}\omega}{4P}\int_{-c}^{c}\int_{-d}^{d}\Delta u_j(y_1, y_2)\sigma_{3j}^{\mathrm{re}}(y_1, y_2)\,\mathrm{d}y_1\,\mathrm{d}y_2, \tag{32}$$

where P is the incident electric power to the probe, Δu_j is the COD due to the incoming field, and $\sigma_{2j}^{\mathrm{re}}$ is the traction with the receiving probe acting as a transmitter in the absence of the crack. The quantity $\delta\Gamma_1$ denotes the extra electric reflection coefficient from the receiving probe due to the presence of the crack; this is essentially the quantity measured in practice.

Inserting the expansion (28) of the COD into (32) yields

$$\delta\Gamma_1 = \frac{\mathrm{i}\omega}{4P}\sum_{j=1}^{3}\sum_{m=1}^{\infty}\sum_{m'=1}^{\infty}\gamma_{jmm'}M_{jmm'}^{\mathrm{re}}, \tag{33}$$

where $M_{jmm'}^{\mathrm{re}}$ is determined from the traction on the position of the crack with the receiver acting as a transmitter in the absence of a crack. For a transducer acting in pulse-echo mode it is, of course, not necessary to distinguish between the transmitter and the receiver.

Though the change in signal response due to the crack is the key quantity in a practical case, it may be of some interest to consider the effect of the interface separately. Using Auld's approach an expression for the difference in signal response between the structure without a crack and a half-space can be derived:

$$\begin{aligned}\delta\Gamma_2 = \frac{\mathrm{i}\omega}{4P}(2\pi)^2\sum_{l,l'=-\infty}^{\infty}\sum_{n=1}^{3}\int_{-\pi/a}^{\pi/a}\int_{-\infty}^{\infty}\xi_{nl}^{\mathrm{re}}\mathrm{e}^{-\mathrm{i}[q_l(x_{\mathrm{r}}+a_{\mathrm{c}})+py_{\mathrm{r}}+h_{nl}^{1-}d_1]}\\ \times\Bigg[\left(\frac{2\pi(l-l')}{ah_{nl}^{1-}}\mathrm{J}_{l'-l}(h_{nl}^{1-}b)S_{n1jl}^{1-}+\mathrm{J}_{l'-l}(h_{nl}^{1-}b)S_{n3jl}^{1-}\right)\alpha_j\left(-q_0-l'\frac{2\pi}{a},-p\right)\\ -U_{njl}^{1-}\mathrm{J}_{l'-l}(h_{nl}^{1-}b)\beta_j\left(-q_0-l'\frac{2\pi}{a},-p\right)\Bigg]\mathrm{d}q_0\,\mathrm{d}p.\end{aligned} \tag{34}$$

Here ξ_{nl}^{re} are the coefficients of (25) with the receiver acting as a transmitter, $(x_{\mathrm{r}}, y_{\mathrm{r}}, d_1)$ are the coordinates of the receiver, and α_j, β_j are determined from (27).

7. Numerical results

There are numerous parameters that can be varied in this problem. Here some numerical results that illustrate the effect of the interface and the crack will be given. The base material 1 has a thickness $d_1 = 30$ mm and is regarded as an isotropic steel with density $\rho^1 = 8.40$ g/cm^3, and with longitudinal and transverse wave velocities 5.90 mm/μs and 3.20 mm/μs, respectively. The cladding has a thickness $d_2 = 5$ mm and is assumed to be a transversely isotropic steel with density $\rho^2 = 8.50$ g/cm^3 and stiffness constants (in GPa) $C_{11}^2 = 216$, $C_{22}^2 = C_{33}^2 = 250$, $C_{12}^2 = C_{13}^2 = 115$, and $C_{44}^2 = 100$, all in abbreviated notation. Only the case where the crystal axes coincide with the $x_1x_2x_3$-axes have been considered in the numerical examples. Damping in the materials is modeled by adding a small imaginary part, 2% of the real part, to all stiffnesses. It should be noted, however, that Auld's reciprocity relation is strictly

valid only for lossless media, which means that the present numerical results are approximate in that sense. The interface between the base material and the cladding is taken as sinusoidal according to (3) with $a = 5$ mm. Reflection from the scan surface $x_3 = d_1$ has been neglected in all numerical examples. The transmitter is of SV type working in pulse echo mode with an angle of 45°, and the size is 10 by 10 mm. Only the case of a fixed frequency, 1 or 2 MHz, has been studied. All results are calibrated with a side-drilled hole of diameter 3 mm and depth 33 mm.

When calculating the matrices Z and M from (52) and (53), it is necessary to truncate the infinite integrals. For the first two terms in matrix Z this has already been accomplished in [Boström et al. 2003], and the reader is referred to that paper for details. For the infinite integrals in the third term of Z and in M it was found that it is sufficient to evaluate the integrals from $-N$ to N, where $N = c_{\mathrm{s,cl}}/2c_{\mathrm{s,b}}$. Here $c_{\mathrm{s,cl}} = \sqrt{C_{44}^2/\rho^2}$ is a typical shear wave velocity in the cladding, and $c_{\mathrm{s,b}}$ is the shear wave velocity in the base material. Increasing N further above this value will not change the final result significantly. The sums over subscripts l and l' in the third term of matrix Z also need to be truncated. By experimenting numerically it has been found that the maximum value of l may be taken as $l_{\max} = \max(k_{s,\mathrm{cl}}a - 3, 4)$, where $k_{s,\mathrm{cl}} = 2\pi f/c_{\mathrm{s,cl}}$ is the shear wave number in the cladding. In the same way it is necessary to truncate the summation over subscripts m and m' in (32). Using $m_{\max} = 2k_{s,\mathrm{cl}}/3+4$ it is seen that the convergence will be sufficient. With the truncations chosen the accuracy is well below 0.1 dB, which corresponds to about 1 per cent in the amplitude of the signal measured. For comparison a difference of about 1-2 dB between simulations and experiments is normally considered as satisfactory in ultrasonic testing. To the author's knowledge there are neither results obtained by alternative methods nor experimental data to compare with for this particular problem.

Figure 2 shows the signal response for a few different sizes of the crack as a function of the position of a 2 MHz transmitter. The crack is "vertical", i.e., $y_1 = -x_3 + d_{\mathrm{c}}$, $y_2 = x_2$, and $y_3 = x_1 - a_{\mathrm{c}}$, and it is located below a valley of the interface ($a_{\mathrm{c}} = 3.75$ mm). The amplitude of the interface is $b = 1$ mm.

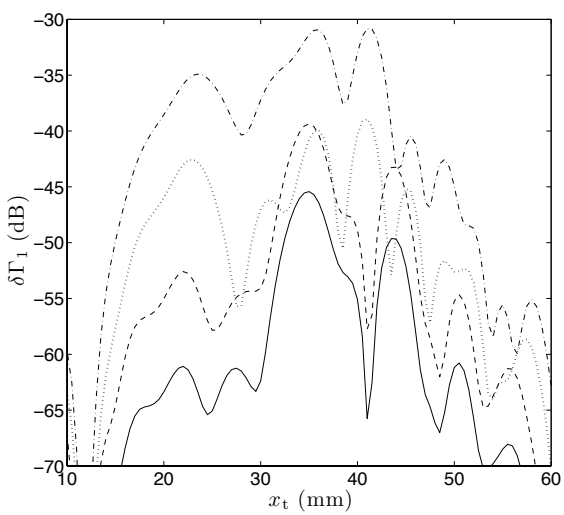

Figure 2. Signal response ($\delta\Gamma_1$) as a function of the position (x_{t}) of a 2 MHz transmitter for different sizes of the crack, 2 × 2 mm (solid), 2 × 4 mm (dashed), 3 × 3 mm (dotted), and 3 × 6 mm (dash-dotted).

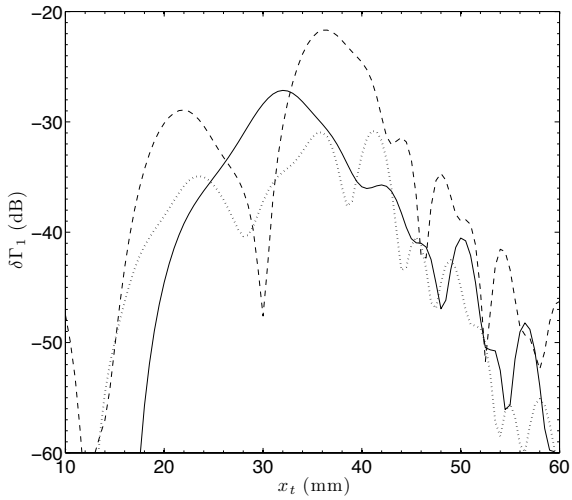

Figure 3. Signal response ($\delta\Gamma_1$) as a function of the position (x_t) of a 2 MHz transmitter for various values of the amplitude of the interface, $b = 0$ (solid), $b = 0.5$ mm (dashed), $b = 1$ mm (dotted).

Figure 3 shows the influence of the amplitude of the interface (b) for the 3×6 mm crack of Figure 2. The same 2 MHz transducer is used. Obviously the amplitude is very important for the signal response. Changing the b from 0.5 to 1 mm gives a decrease of about 9 dB for the maximum value. However, there does not seem to be any simple systematic relation between the amplitude b and the maximum signal response.

Figure 4 shows the effect of translating the crack with respect to the interface for the same transducer as in the previous examples. The positions chosen correspond to a crack centered directly below a top

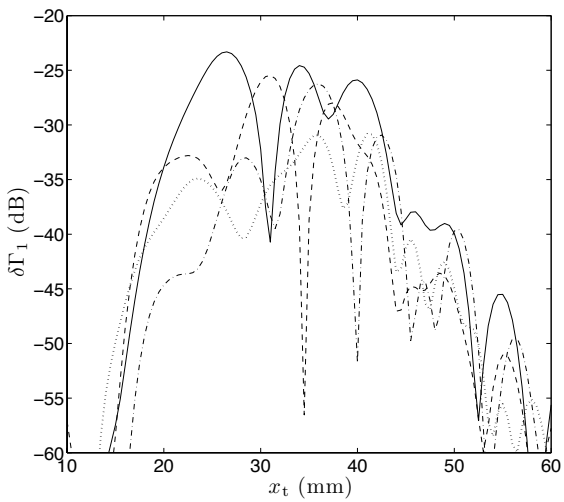

Figure 4. Signal response ($\delta\Gamma_1$) as a function of the position (x_t) of a 2 MHz transmitter for various values of the position of the crack relative to the corrugated interface, $a_c = 1.25$ mm (solid), $a_c = 2.5$ mm (dashed), $a_c = 3.75$ mm (dotted), $a_c = 0$ (dash-dotted).

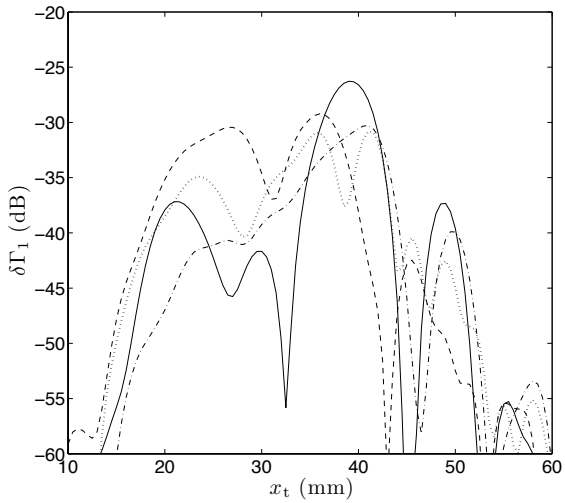

Figure 5. Signal response ($\delta\Gamma_1$) as a function of the position (x_t) of a 2 MHz transmitter for various values of the orientation of the crack, $\varphi = 0$ (horizontal crack, solid), $\varphi = 45°$ (dashed), $\varphi = 90°$ (vertical crack, dotted), $\varphi = 135°$ (dash-dotted).

or a valley of the interface, or in the middle of these two. There does not seem to be any systematic dependence on the position, but it is worth pointing out that there is a difference of about 8 dB between the maximum responses for a crack below a top ($a_c = 1.25$ mm) and a crack directly below a valley ($a_c = 3.75$ mm).

In Figure 5 the response from cracks with varying orientation is examined, still with a 2 MHz transducer. All cracks have a normal (y_3-axis) in the x_1x_3-plane and are rotated an angle φ about the x_2-axis

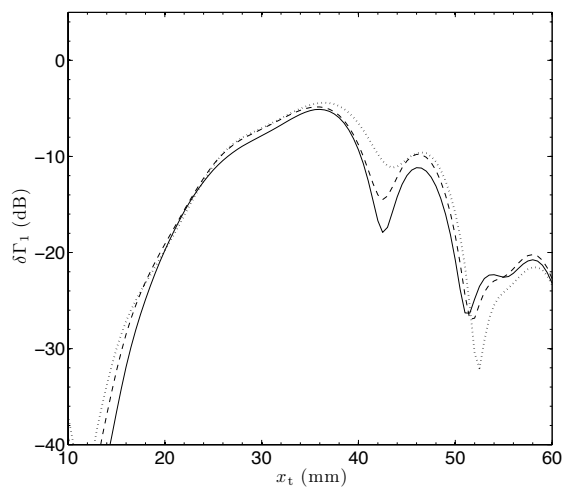

Figure 6. Signal response ($\delta\Gamma_1$) as a function of the position (x_t) of a 1 MHz transmitter for various values of the amplitude of the interface, $b = 0$ (solid), $b = 0.5$ mm (dashed), $b = 1$ mm (dotted).

with $\varphi = 0$ corresponding to the "horizontal" position, where the $y_1y_2y_3$-system is not rotated. The strongest echo is obtained from the horizontal crack, about 5 dB stronger than for the vertical crack.

Finally, in Figure 6 some results for a 1 MHz transducer are shown. Apart from the frequency, all parameters have the same values as in Figure 3. The obvious result is that at low frequencies the wavy interface only has a minor influence on the signal response. Similar results are obtained when the crack is translated sideways as in Figure 4. Tilting the crack, however, give results more in accordance with the 2 MHz case.

8. Concluding remarks

In this paper the effect of a two-dimensional periodic interface on three-dimensional wave scattering by a rectangular crack in a cladding has been investigated. A mathematical model has been developed, where the elastic wave propagation problem is solved exactly. It is seen that the properties of the wavy interface are of major importance for the signal response at higher frequencies. From systematic studies with varying values of the governing parameters it should possible to acquire a deeper understanding of the influence of the properties of the interface, the size, location, and orientation of the crack, the material parameters, etc. It is believed that the model will provide a useful tool for planning and qualification of ultrasonic testing procedures. For instance, it should be possible to judge whether a defect of a certain size, location, and orientation would be possible to detect using a certain method of inspection (transmitter type, frequency, search pattern).

Acknowledgments

This work is sponsored by the Swedish Radiation Safety Authority, and this is gratefully acknowledged.

Appendix A: The half-space Green's tensors

The half space Green's tensor expressed as a double Fourier transform has been derived in [Boström et al. 2003]. To do this plane wave solutions are determined by defining a vector $\boldsymbol{v}^i\,(i = 1, 2)$ as

$$\boldsymbol{v}^i = \left(u_1^i \;\; u_2^i \;\; u_3^i \;\; \sigma_{13}^i \;\; \sigma_{23}^i \;\; \sigma_{33}^i \right)^{\mathrm{T}}, \tag{35}$$

where all elements are assumed to have an $\exp(\mathrm{i}(qx_1 + px_2 + h^i x_3))$ dependence, which is suppressed in the following. Substituting into (1) and (2) leads to a generalized eigenvalue problem

$$A^i \boldsymbol{v}^i = h^i C^i \boldsymbol{v}^i. \tag{36}$$

The explicit expressions for the matrices A^i and C^i are not given here. The reader is referred to [Boström et al. 2003] for details. Solving the eigenvalue problem gives six eigenvalues $h_n^{i\pm}$, $n = 1, 2, 3$, where the superscript indicates propagation in the positive or negative x_3-direction. The corresponding eigenvectors are denoted by

$$\boldsymbol{v}_n^{i\pm} = \left(U_{n1}^{i\pm} \;\; U_{n2}^{i\pm} \;\; U_{n3}^{i\pm} \;\; T_{n1}^{i\pm} \;\; T_{n2}^{i\pm} \;\; T_{n3}^{i\pm} \right)^{\mathrm{T}}. \tag{37}$$

The half-space Green's tensor can then be expressed as a double Fourier transform by adding the free space Green's tensor and a reflected part that is constructed so that the stress-free boundary condition on

the free surface is satisfied. For the base material ($i = 1$) the result is

$$G^1_{jj'}(\boldsymbol{x};\boldsymbol{x}') = \int_{-\infty}^{\infty}\int_{-\infty}^{\infty}\sum_{n=1}^{3} D_n^{1\pm}U_{nj'}^{1\pm}U_{nj}^{1\pm}\,\mathrm{e}^{\mathrm{i}(q(x_1-x_1')+p(x_2-x_2')+h_n^{1\pm}(x_3-x_3'))}\,\mathrm{d}q\,\mathrm{d}p$$
$$+\int_{-\infty}^{\infty}\int_{-\infty}^{\infty}\sum_{n,n'=1}^{3} D_n^{1+}U_{nj'}^{i+}B_{nn'}^{1}U_{n'j}^{1-}\,\mathrm{e}^{\mathrm{i}(q(x_1-x_1')+p(x_2-x_2')+h_{n'}^{1-}(x_3-d_1)-h_n^{1+}(x_3'-d_1))}\,\mathrm{d}q\,\mathrm{d}p, \quad (38)$$

for $x_3 \gtrless x_3'$. The quantities $D_n^{i\pm}$ are determined by the jump condition for the free space Green's tensor at $x_3 = x_3'$. This leads to

$$\sum_{n=1}^{3}(D_n^{i+}U_{nj}^{i+}U_{nj'}^{i+} - D_n^{i-}U_{nj}^{i-}U_{nj'}^{i-}) = 0, \quad (39)$$

$$\sum_{n=1}^{3}(D_n^{i+}T_{nj}^{i+}U_{nj'}^{i+} - D_n^{i-}T_{nj}^{i-}U_{nj'}^{i-}) = -\delta_{jj'}/(2\pi)^2. \quad (40)$$

Obviously, there are 18 equations and 6 unknowns for each material. However, the equations are not linearly independent, since the symmetry properties of the Green's tensor have already been exploited. The reflection matrix B^i is determined from the condition that the traction vanishes on the free surface, which means that

$$T_{nj}^{1+} + \sum_{n'=1}^{3} B_{nn'}^{1}T_{n'j}^{1-} = 0, \quad (41)$$

$$T_{nj}^{2-} + \sum_{n'=1}^{3} B_{nn'}^{2}T_{n'j}^{2+} = 0, \quad (42)$$

for $n, j = 1, 2, 3$.

Appendix B: The matrices Q^i and P^i

If reflection at the scan surface S_1 is neglected, and the interface is taken as sinusoidal,

$$s(x_1) = b\sin\frac{2\pi x_1}{a}, \quad (43)$$

then the explicit expressions for the matrices $Q^1, \ldots, Q^4$, P^3, P^4 are

$$Q^1_{nljl'} = A^{1-}_{nljl'}\mathrm{e}^{\mathrm{i}h_{nl}^{1-}d_1}, \quad (44)$$

$$Q^2_{nljl'} = C^{1-}_{nljl'}\mathrm{e}^{\mathrm{i}h_{nl}^{1-}d_1}, \quad (45)$$

$$Q^3_{nljl'} = A^{2+}_{nljl'} + \sum_{n'=1}^{3} A^{2-}_{n'ljl'}B^{2}_{n'nl}\mathrm{e}^{\mathrm{i}d_2(h_{nl}^{2+}-h_{n'l}^{2-})}, \quad (46)$$

$$Q^4_{nljl'} = C^{2+}_{nljl'} + \sum_{n'=1}^{3} C^{2-}_{n'ljl'}B^{2}_{n'nl}\mathrm{e}^{\mathrm{i}d_2(h_{nl}^{2+}-h_{n'l}^{2-})}, \quad (47)$$

$$P^3_{nljl'} = A^{2-}_{nljl'}, \tag{48}$$

$$P^4_{nljl'} = C^{2-}_{nljl'}, \tag{49}$$

where

$$A^{i\pm}_{nkljl'} = 2\pi\left(\frac{2\pi(l-l')}{h^{i\pm}_{nl}} S^{i\pm}_{n1jl} + aS^{i\pm}_{n3jl}\right) \mathrm{J}_{l'-l}(bh^{i\pm}_{nl}) D^{i\pm}_{nl}, \tag{50}$$

$$C^{i\pm}_{nljl'} = 2\pi a U^{i\pm}_{njl} \mathrm{J}_{l'-l}(bh^{i\pm}_{nl}) D^{i\pm}_{nl}. \tag{51}$$

Appendix C: The matrices Z and M

The explicit expressions for the matrices Z and M from (31) are

$$\begin{aligned}
&Z_{jmm'j'm''m'''} \\
&= (-1)^{m''+m'''} mm'm''m''' \int_{-\infty}^{\infty}\int_{-\infty}^{\infty} \sum_{n=1}^{3} D^{\mathrm{c}-}_n S^{\mathrm{c}-}_{nj} S^{\mathrm{c}-}_{nj'} \frac{\mathrm{J}_m(qc)\mathrm{J}_{m'}(pd)\mathrm{J}_{m''}(qc)\mathrm{J}_{m'''}(pd)}{q^2p^2}\,\mathrm{d}q\,\mathrm{d}p \\
&\quad + (-1)^{m''+m'''} mm'm''m''' \int_{-\infty}^{\infty}\int_{-\infty}^{\infty} \sum_{n,n'=1}^{3} D^{2-}_n S^{2\mathrm{c}-}_{nj} B^2_{nn'} S^{2\mathrm{c}+}_{n'j'} \\
&\qquad\qquad \times \frac{\mathrm{J}_m(\lambda^-_{1n}c)\mathrm{J}_{m'}(\lambda^-_{2n}d)\mathrm{J}_{m''}(\lambda^+_{1n'}c)\mathrm{J}_{m'''}(\lambda^+_{2n'}d)}{\lambda^-_{1n}\lambda^-_{2n}\lambda^+_{1n'}\lambda^+_{2n'}} \mathrm{e}^{\mathrm{i}(h^{2+}_{n'}-h^{2-}_n)(d_2-d_\mathrm{c})}\,\mathrm{d}q\,\mathrm{d}p \\
&\quad + (-1)^{m''+m'''} mm'm''m''' \sum_{l,l'=-\infty}^{\infty} \int_{-\pi/a}^{\pi/a}\int_{-\infty}^{\infty} \sum_{n,n'=1}^{3} A_{nln'l'} \\
&\qquad \times \left(S^{2\mathrm{c}-}_{nj'l} \frac{\mathrm{J}_{m''}(\lambda^-_{1nl}c)\mathrm{J}_{m'''}(\lambda^-_{2nl}d)}{\lambda^-_{1nl}\lambda^-_{2nl}} \mathrm{e}^{-\mathrm{i}h^{2-}_{nl}d_\mathrm{c}} + \sum_{n''=1}^{3} B^2_{nn''l} S^{2\mathrm{c}+}_{n''j'l} \frac{\mathrm{J}_{m''}(\lambda^+_{1n''l}c)\mathrm{J}_{m'''}(\lambda^+_{2n''l}d)}{\lambda^+_{1n''l}\lambda^+_{2n''l}} \mathrm{e}^{\mathrm{i}[h^{2+}_{n''l}(d_2-d_\mathrm{c})-h^{2-}_{nl}d_2]} \right) \\
&\qquad \times \left(D^{2+}_{n'l'} S^{2\mathrm{c}+}_{n'jl'} \frac{\mathrm{J}_m(\lambda^+_{1n'l'}c)\mathrm{J}_{m'}(\lambda^+_{2n'l}d)}{\lambda^+_{1n'l'}\lambda^+_{2n'l'}} \mathrm{e}^{\mathrm{i}h^{2+}_{n'l'}d_\mathrm{c}} \right. \\
&\qquad\qquad \left. + \sum_{n'''=1}^{3} D^{2-}_{n'''l'} B^2_{n'''n'l'} S^{2\mathrm{c}-}_{n'''j'l'} \frac{\mathrm{J}_m(\lambda^-_{1n'''l'}c)\mathrm{J}_{m'}(\lambda^-_{2n'''l'}d)}{\lambda^-_{1n'''l'}\lambda^+_{2n'''l'}} \mathrm{e}^{\mathrm{i}[-h^{2-}_{n'''l'}(d_2-d_\mathrm{c})+h^{2+}_{n'l'}d_2]} \right) \mathrm{e}^{2\pi\mathrm{i}(l-l')a_\mathrm{c}/a}\,\mathrm{d}q_0\,\mathrm{d}p.
\end{aligned} \tag{52}$$

It should be noted that the first two terms in the matrix Z correspond to scattering from a rectangular crack in a homogeneous anisotropic medium, which is the problem solved in [Boström et al. 2003]. Thus, it is only the third term, describing the influence of the cladding, which needs to be calculated.

$$\begin{aligned}
M_{jmm'} &= (-1)^{(m+m')} mm' \sum_{n,n'=1}^{3} \sum_{l,l'=-\infty}^{\infty} \int_{-\pi/a}^{\pi/a}\int_{-\infty}^{\infty} g_{nl} \mathrm{e}^{\mathrm{i}q_l a_\mathrm{c}} \\
&\times \left(S^{2\mathrm{c}-}_{njl} \frac{\mathrm{J}_m(\lambda^-_{1nl}c)\mathrm{J}_{m'}(\lambda^-_{2nl}d)}{\lambda^-_{1nl}\lambda^-_{2nl}} \mathrm{e}^{-\mathrm{i}h^{2-}_{nl}d_\mathrm{c}} + \sum_{n'=1}^{3} B^2_{nn'l} S^{2\mathrm{c}+}_{n'jl} \frac{\mathrm{J}_m(\lambda^+_{1n'l}c)\mathrm{J}_{m'}(\lambda^+_{2n'l}d)}{\lambda^+_{1n'l}\lambda^+_{2n'l}} \mathrm{e}^{\mathrm{i}[h^{2+}_{n'l}(d_2-d_\mathrm{c})-h^{2-}_{nl}d_2]} \right) \mathrm{d}q_0\,\mathrm{d}p.
\end{aligned} \tag{53}$$

References

[Auld 1979] B. A. Auld, "General electromechanical reciprocity relations applied to the calculation of elastic wave scattering coefficients", *Wave Motion* **1**:1 (1979), 3–10.

[Boström and Wirdelius 1995] A. Boström and H. Wirdelius, "Ultrasonic probe modeling and nondestructive crack detection", *J. Acoust. Soc. Am.* **97**:5 (1995), 2836–2848.

[Boström et al. 2003] A. Boström, T. Grahn, and A. J. Niklasson, "Scattering of elastic waves by a rectangular crack in an anisotropic half-space", *Wave Motion* **38**:2 (2003), 91–107.

[Fokkema 1980] J. T. Fokkema, "Reflection and transmission of elastic waves by the spatially periodic interface between two solids (theory of the integral-equation method)", *Wave Motion* **2**:4 (1980), 375–393.

[Fokkema and van den Berg 1977] J. T. Fokkema and P. M. van den Berg, "Elastodynamic diffraction by a periodic rough surface (stress-free boundary)", *J. Acoust. Soc. Am.* **62**:5 (1977), 1095–1101.

[Hudgell 1994] R. J. Hudgell, *Handbook on the ultrasonic examination of austenitic clad steel components*, EUR **15786**, Office for Official Publications of the European Communities, Luxembourg, 1994.

[Jansson 2010] P.-Å. Jansson, "Scattering from a rectangular crack in a cladding", pp. 383–388 in *IUTAM Symposium on Recent Advances of Acoustic Waves in Solids* (Taipei, 2009), edited by T.-T. Wu and C.-C. Ma, IUTAM Bookseries **26**, Springer, New York, 2010.

[Jansson and Zagbai 2007] P.-Å. Jansson and T. Zagbai, "2D P-SV wave scattering by a crack in a cladding", pp. 71–78 in *Review of progress in quantitative nondestructive evaluation* (Portland, OR, 2006), edited by D. O. Thompson and D. E. Chimenti, AIP Conference Proceedings **894**, American Institute of Physics, Melville, NY, 2007.

[Krasnova 2005] T. Krasnova, *Elastic wave scattering from corrugated surfaces in anisotropic media*, Ph.D. thesis, Chalmers University of Technology, Gothenburg, 2005.

[Krasnova and Jansson 2006] T. Krasnova and P.-Å. Jansson, "Wave scattering from a slightly wavy interface between two anisotropic media", *J. Nondestruct. Eval.* **25**:4 (2006), 155–164.

[Krasnova et al. 2005] T. Krasnova, P.-Å. Jansson, and A. Boström, "Ultrasonic wave propagation in an anisotropic cladding with a wavy interface", *Wave Motion* **41**:2 (2005), 163–177.

[Lakhtakia et al. 1984] A. Lakhtakia, V. K. Varadan, V. V. Varadan, and D. J. N. Wall, "The T-matrix approach for scattering by a traction-free periodic rough surface", *J. Acoust. Soc. Am.* **76**:6 (1984), 1839–1846.

[Langenberg et al. 2000] K. J. Langenberg, R. Hannemann, T. Kaczorowski, R. Marklein, B. Koehler, C. Schurig, and F. Walte, "Application of modeling techniques for ultrasonic austenitic weld inspection", *NDT & E Int.* **33**:7 (2000), 465–480.

[Liu and Achenbach 1995] G. R. Liu and J. D. Achenbach, "Strip element method to analyze wave scattering by cracks in anisotropic laminated plates", *J. Appl. Mech.* (*ASME*) **62**:3 (1995), 607–613.

[Niklasson 1998] A. J. Niklasson, "Ultrasonic three-dimensional probe modeling in anisotropic solids", *J. Acoust. Soc. Am.* **103**:5 (1998), 2432–2442.

[Richtmyer 1981] R. D. Richtmyer, *Principles of advanced mathematical physics*, vol. 1, Springer, New York, 1981.

[Wang et al. 1996] C.-Y. Wang, J. D. Achenbach, and S. Hirose, "Two-dimensional time domain BEM for scattering of elastic waves in solids of general anisotropy", *Int. J. Solids Struct.* **33**:26 (1996), 3843–3864.

[Zagbai and Boström 2006] T. Zagbai and A. Boström, "2D SH wave scattering by a crack in a cladding", pp. 81–88 in *Review of progress in quantitative nondestructive evaluation* (Brunswick, ME, 2005), edited by D. O. Thompson and D. E. Chimenti, AIP Conference Proceedings **820**, American Institute of Physics, Melville, NY, 2006.

Received 21 Sep 2010. Revised 15 Feb 2011. Accepted 20 Mar 2011.

PER-ÅKE JANSSON: per-ake.jansson@chalmers.se
Department of Applied Mechanics, Chalmers University of Technology, SE-412 96 Gothenburg, Sweden

JOURNAL OF MECHANICS OF MATERIALS AND STRUCTURES

jomms.org

Founded by Charles R. Steele and Marie-Louise Steele

See http://jomms.org for submission guidelines.

JoMMS (ISSN 1559-3959) is published in 10 issues a year. The subscription price for 2011 is US $520/year for the electronic version, and $690/year (+$60 shipping outside the US) for print and electronic. Subscriptions, requests for back issues, and changes of address should be sent to Mathematical Sciences Publishers, Department of Mathematics, University of California, Berkeley, CA 94720–3840.

JoMMS peer-review and production is managed by EditFLOW® from Mathematical Sciences Publishers.

PUBLISHED BY
mathematical sciences publishers
http://msp.org/

A NON-PROFIT CORPORATION

Typeset in LaTeX

Journal of Mechanics of Materials and Structures
Volume 6, No. 9-10 November–December 2011